Fluctuations and Symmetry Energy in Nuclear Fragmentation Dynamics

M. Colonna

INFN-Laboratori Nazionali del Sud, I-95125 Catania, Italy

Within a dynamical description of nuclear fragmentation, based on the liquid-gas phase transition scenario, we explore the relation between neutron-proton density fluctuations and nuclear symmetry energy. We show that, along the fragmentation path, isovector fluctuations follow the evolution of the local density and approach an equilibrium value connected to the local symmetry energy. Higher-density regions are characterized by smaller average asymmetry and narrower isotopic distributions. This dynamical analysis points out that fragment final state isospin fluctuations can probe the symmetry energy of the density domains from which fragments originate.

The dynamics and thermodynamics of complex systems present general aspects of interest in different domains of physics. A rather important issue is the identification of the occurrence of phase transitions. This is relevant for many microscopic or mesoscopic systems, from metallic clusters to Bose condensates and nuclei [1–3]. In particular, the analysis of two-component systems has recently evidenced new interesting features [4–7].

Under suitable conditions of density and temperature, the nuclear equation of state (EOS) foresees the possibility of phase transitions from liquid to vapor phases, a scenario often evoked to explain the multifragmentation phenomenon [8–10]. As a consequence of the two-component structure of nuclear matter, constituted by protons and neutrons, a crucial role is played by the low-density behavior of the isovector part of the interaction and the corresponding term in the nuclear EOS, the symmetry energy [11], on which many investigations are concentrated [12–16]. We stress that this information is essential in the astrophysical context, for the understanding of the properties of compact objects such as neutron stars whose crust behaves as low-density asymmetric nuclear matter [17,18]. Moreover, the density dependence of the symmetry energy affects the structure of exotic nuclei and the appearance of new features involving the neutron skin [19].

A connection between the characteristics of clusters emerging from nuclear fragmentation and the symmetry energy has been proposed in the framework of macroscopic statistical models [20–22]. However, it would be important to explore this issue within a full dynamical description of the fragmentation process. Here we undertake such study for systems facing low-density (spinodal) instabilities and first-order phase transitions [11]. We investigate the coupling between the development of neutron-proton density fluctuations (isovector fluctuations), to which isotopic properties are connected, and the growth of unstable modes of the total density, leading to the formation of nuclear drops (fragments). Thus the aim of this work is to examine the behavior of isovector

fluctuations in rapidly evolving systems to probe their possible relation to the symmetry energy and its density dependence.

Theoretically the evolution of complex systems can be described by a one-body transport equation with a fluctuating term that incorporates the effects of the unknown many-body correlations, the so-called Boltzmann-Langevin equation [23,24]. We follow the approximate treatment of the Boltzmann-Langevin equation presented in Ref. [25], the stochastic mean-field model. We solve the following equation for the time evolution of the semiclassical one-body distribution function $f(\boldsymbol{r}, \boldsymbol{p}, t)$:

$$\frac{\partial f}{\partial t} + \boldsymbol{v}\frac{\partial f}{\partial \boldsymbol{r}} - \frac{\partial U}{\partial \boldsymbol{r}}\frac{\partial f}{\partial \boldsymbol{p}} = \bar{I}_{\text{coll}}[f] + \frac{\partial U_{\text{ext}}}{\partial \boldsymbol{r}}\frac{\partial f}{\partial \boldsymbol{p}}, \quad (1)$$

where $U[\rho]$ is the self-consistent mean-field potential, $\bar{I}_{\text{coll}}[f]$ is the average collision integral, and $U_{\text{ext}}(\boldsymbol{r})$ represents an external, stochastic field. The coordinates of isospin are not shown for brevity. Within such a framework, the effective nuclear potential U is derived from energy functionals that usually contain a term proportional to I^2, the symmetry energy $E_{\text{sym}}(\rho, I)/A \equiv C_{\text{sym}}(\rho)I^2$ [with $I \equiv (\rho_n - \rho_p)/\rho$ and ρ, ρ_n, ρ_p denoting total, neutron, and proton densities, respectively].

Let us consider the behavior of nuclear matter prepared with a uniform density distribution ρ_0 and with a Fermi-Dirac momentum distribution corresponding to a specified temperature T. The system is confined within a cubic box, with side $L = 19$ fm, with periodic boundary conditions imposed. The linear response analysis allows one to get a first insight into the fluctuation dynamics. For two-component matter one can identify two types of independent modes of the phase-space density: isoscalarlike modes, where neutrons and protons oscillate in phase, and isovectorlike modes, with neutrons and protons oscillating out of phase. In particular, in the case of symmetric nuclear matter, the two types of modes correspond to oscillations of $f^s = f_n + f_p$ (isoscalar modes) and of $f^v = f_n - f_p$ (isovector modes). Let us denote by

$f_{\mathbf{k}}^q(\boldsymbol{p}, t)$ $(q = s, v)$ the Fourier transform, with respect to $\boldsymbol{r}$, of the difference $\delta f^q = f^q - f_0^q$, where f_0^q is the system initial phase-space density. The equation of motion for these Fourier coefficients follows readily from (1),

$$\frac{\partial}{\partial t} f_{\mathbf{k}}^q + i\mathbf{k} \cdot \boldsymbol{v} f_{\mathbf{k}}^q - i\frac{\partial U_k^q}{\partial \rho^q} \mathbf{k} \cdot \boldsymbol{v} \frac{\partial f_0}{\partial \epsilon} \rho_{\mathbf{k}}^q = i\mathcal{F}_{\mathbf{k}}^q \mathbf{k} \cdot \boldsymbol{v} \frac{\partial f_0}{\partial \epsilon}.$$

(2)

Here, $\partial U_k^q / \partial \rho^q$ represents the appropriate Fourier component of the derivative of the effective field with respect to the density ρ^q and $\mathcal{F}_{\mathbf{k}}^q(t)$ is the Fourier component of the external field. Furthermore, $\rho_{\mathbf{k}}^q(t)$ is the Fourier transform of the density fluctuation $\delta\rho^q(\boldsymbol{r})$. Finally, since we will restrict our analysis to rather low temperatures, in Eq. (2) we have ignored the average collision term $\bar{I}_{\mathrm{coll}}$, since its effect is relatively small [26].

For stable modes, the equilibrium variance σ_k^q associated with the fluctuation $\rho_{\mathbf{k}}^q$ is linked to the physical quantities that characterize the response of the system to the action of the external force $\mathcal{F}_{\mathbf{k}}^q$; see Eq. (2). According to the fluctuation-dissipation theorem [27], one can write $\sigma_k^q = T/F^q(k)$, where $F^q(k) = (\frac{\partial U_k^q}{\partial \rho^q} + 1/\mathcal{N})$, with $\mathcal{N} = -\frac{4}{(2\pi)^3} \int d\boldsymbol{p} \frac{\partial f_0}{\partial \epsilon}$. We notice that F^q is just the second derivative of the system free energy density with respect to the density ρ^q. Considering the inverse Fourier transform of $\rho_{\mathbf{k}}^q$, we obtain, for the equilibrium spatial density correlations, in a cell of volume ΔV,

$$\sigma_{\rho^q}^{(\mathrm{eq})}(\Delta V) \equiv \langle \delta\rho^q(\boldsymbol{r})\delta\rho^q(\boldsymbol{r})\rangle$$
$$= \frac{1}{(2\pi)^3} \sum_{\mathbf{k}} \sigma_k^q d\mathbf{k} = \frac{T}{\Delta V}\langle 1/F^q(k)\rangle_{\mathbf{k}}, \quad (3)$$

where the average extends over all $\mathbf{k}$ modes.

Focusing on isovector modes, the potential U_k^v represents the Fourier transform of the symmetry potential $U_{\mathrm{sym}}[\rho_0(\boldsymbol{r})] = 2\frac{\rho_v}{\rho_0} \int d\boldsymbol{r}' C_{\mathrm{sym}}^{\mathrm{pot}}[\rho_0(\boldsymbol{r}')]g_\sigma(|\boldsymbol{r} - \boldsymbol{r}'|)$, where $C_{\mathrm{sym}}^{\mathrm{pot}}$ denotes the potential part of C_{sym}, and the smearing function g_σ is introduced to account for the finite range of the nuclear interaction. Thus, we obtain $F^v(k) = 2C_{\mathrm{sym}}^{\mathrm{pot}}(\rho_0)g_\sigma(k)/\rho_0 + 1/\mathcal{N} \equiv 2F_{\mathrm{sym}}(k)/\rho_0$. We note that the function $\mathbf{F}_{\mathrm{sym}}(\rho_0) \equiv F_{\mathrm{sym}}(k=0)$ simply coincides with the volume symmetry free energy that at zero temperature reduces to the symmetry energy $C_{\mathrm{sym}}(\rho_0)$. We can write

$$\langle 1/F^v(k)\rangle_{\mathbf{k}} = \frac{\rho_0}{2}\langle 1/F_{\mathrm{sym}}(k)\rangle_{\mathbf{k}} \equiv \frac{\rho_0}{2F_{\mathrm{eff}}^v}. \quad (4)$$

Hence we find that equilibrium fluctuations of the isovector density can be connected to an "effective" symmetry free energy F_{eff}^v that, owing to the k dependence of the symmetry potential, is smaller than the free energy $\mathbf{F}_{\mathrm{sym}}$.

In asymmetric matter, the findings discussed above still hold for isoscalarlike and isovectorlike oscillations.

Now let us go back to the full nonlinear equations (1) that are solved numerically with the test particle method [28]. We have performed stochastic mean-field calculations for nuclear matter prepared at initial temperature $T = 3$ MeV and in several density conditions. Here we also take account of fluctuations in the isovector channel, which were neglected in Refs. [28,29]. Isovector fluctuations can be extracted from the model by simply rescaling the variance by the number of test particles employed in the simulation [30].

We adopt momentum-independent effective interactions corresponding to a soft EOS, with compressibility modulus $K = 200$ MeV. The coefficient C_{sym} gets a kinetic contribution just from basic Pauli correlations and a potential part, $C_{\mathrm{sym}}^{\mathrm{pot}}$, from the isospin dependence of the interaction. For the local density (ρ) dependence of $C_{\mathrm{sym}}^{\mathrm{pot}}$ we consider two representative parametrizations: one with a linearly increasing behavior with density (asy-stiff), $C_{\mathrm{sym}}^{\mathrm{pot}}(\rho) = 90\rho$ (MeV), and one with a kind of saturation above normal density (asy-soft), $C_{\mathrm{sym}}^{\mathrm{pot}}(\rho) = \rho(238-1009\rho)$ (MeV) [28,29]. We notice that at the temperature considered in the calculation, which is within the typical range observed in multifragmentation [10], the symmetry energy C_{sym} is very close to $\mathbf{F}_{\mathrm{sym}}$. As smearing function g_σ, we take a Gaussian with width $\sigma = 0.9$ fm. With this choice, for nuclear matter at saturation density ($\rho_0 = \rho_{\mathrm{sat}} = 0.145$ fm^{-3}), Eq. (4) gives $F_{\mathrm{eff}}^v = 0.7\mathbf{F}_{\mathrm{sym}}$.

Let us consider first, for the sake of simplicity, the case of symmetric matter ($I = 0$). We first concentrate on isovector fluctuations for uniform matter at rest, where equilibrium conditions are fulfilled. Thus, in order to avoid the development of volume instabilities at low density [11], we switch off in the calculations the isoscalar part of the nuclear potential. Then we calculate the isovector fluctuation variance $\sigma_{\rho^v} = \langle (\delta\rho_n(\boldsymbol{r}) - \delta\rho_p(\boldsymbol{r}))^2\rangle$, where the average is performed over cells of volume $\Delta V = 1$ fm^3. The effective symmetry free energy can be extracted from the numerical variance exploiting Eqs. (3) and (4). This quantity is displayed in Fig. 1(a) as a function of the matter density, for the two parametrizations of the symmetry energy introduced above (thick lines, full for asy-stiff and dashed for asy-soft), and compared with the corresponding symmetry free energy $\mathbf{F}_{\mathrm{sym}}$. The numerical results generally go with the analytical estimation discussed above: Owing to the k dependence of the symmetry potential, the extracted F_{eff}^v is lower than the symmetry free energy, being reduced by about 30% at saturation density, and exhibits a density dependence connected to the asy-stiffness of the effective interaction employed in the simulations.

The evaluation of the equilibrium isovector fluctuations of stable matter can be used as a benchmark for the general and more interesting case where unstable systems are allowed to evolve. Calculations have been performed taking, as initial density ρ_0, three values inside the spinodal
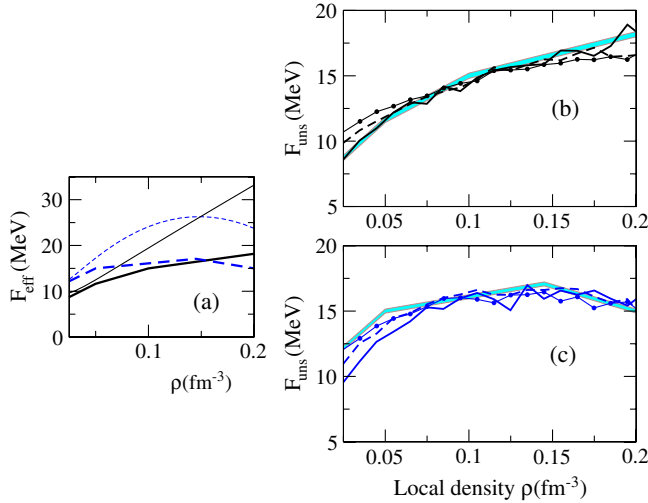
FIG. 1 (color online). (a) The quantity F_{eff}^v, extracted from stochastic mean-field simulations, for stable nuclear matter in several density conditions and at temperature $T = 3$ MeV (thick lines). Thin lines show the density dependence of the symmetry free energy $\mathbf{F}_{\text{sym}}$. Full lines, asy-stiff EOS; dashed lines, asy-soft EOS. (b) The quantity F_{uns}^v as a function of the local density for unstable systems with initial density ρ_1 (full lines), ρ_2 (dashed lines), ρ_3 (dotted lines), asy-stiff EOS. (c) Same as in (b) for asy-soft EOS. In (b) and (c) thick gray (cyan) lines represent the same results shown in (a) as thick lines.

region: $\rho_1 = 0.0245$ fm^{-3}, $\rho_2 = 2\rho_1$, and $\rho_3 = 3\rho_1$. Moreover, for each case, we have considered symmetric matter [system (1), $I_1 = 0$] and asymmetric matter [system (2), $I_2 = 0.142$].

Now the system may develop density fluctuations, so locally the density gets larger (density bumps, leading to fragments) or smaller (vapor) than the initial value [11]. The separation between the two regimes is smooth, so that the local density ρ may vary between zero and values around the saturation density. Our analysis is performed at the "freeze-out" time $t = 200$ fm/c, when isoscalar density fluctuations saturate. At this time, the average density of the regions having ρ larger than ρ_0 goes from 0.064 fm^{-3} (in the ρ_1 case) to 0.10 fm^{-3} (ρ_2 case) and 0.12 fm^{-3} (ρ_3 case).

Our aim is to investigate the behavior of isovector fluctuations on the short time scale (the freeze-out time) associated with fragment formation. Isovector fluctuations are evaluated as a function of the local density inside the fragmenting system, looking at the variance of the isovector density ρ^v in cells having the same local density ρ. As a measure of the isovector variance σ_{ρ^v}, we consider the quantity $F_{\text{uns}}^v = (\rho T)/(2\Delta V \sigma_{\rho^v})$ that coincides with F_{eff}^v if equilibrium is reached [see Eqs. (3) and (4)]. Results for F_{uns}^v, obtained in the case of symmetric matter, are displayed in Fig. 1 as a function of the local density for the three initial density values considered; Figs. 1(b) and 1(c). Quite interestingly, isovector fluctuations follow the local

value of the symmetry energy independently of the initial conditions of the system. Indeed the three curves associated with the different initial densities (full, dashed, and dotted lines for ρ_1, ρ_2, and ρ_3, respectively) are rather close to each other and they are also close, for each given local density, to the equilibrium results discussed above [here plotted as thick gray (cyan) lines]; thus, locally, $F_{\text{uns}}^v \approx F_{\text{eff}}^v$. These results indicate that, as soon as density fluctuations start to develop, a quick rearrangement of isovector fluctuations takes place, so that the equilibrium value corresponding to the new actual local density is approached. Indeed, isovectorlike oscillations are characterized by a much shorter time scale, with respect to the growth of the unstable modes [31]. Thus, important coupling effects between isoscalar and isovector oscillations are emerging from the solution of the full nonlinear equations (1).

Calculations have also been performed for the asymmetric system (2), leading to results very close to the ones displayed in Fig. 1. In the latter case one can also discuss the isospin distillation mechanism that induces a deviation of the local asymmetry from the system initial value [29]. In particular, we consider the following density-dependent quantity, derived from the symmetric system (1) and the asymmetric system (2): $\Delta(\overline{Z/A})^2 = (\overline{Z/A})_1^2 - (\overline{Z/A})_2^2$, where $(\overline{Z/A})_i$ (with $i = 1, 2$) represents for system (i) the average proton fraction of cells having the same local density ρ. This quantity is displayed in Fig. 2 as a function of ρ. The different curves correspond to the two EOS [gray (red) lines for soft, black lines for stiff] and the three initial densities considered. As a general trend, we observe the well-known behavior of asymmetric systems: The low-density regions become more neutron rich, while high-density regions are more symmetric, just in connection with the density dependence of the symmetry energy coefficient $C_{\text{sym}}(\rho)$. Here what is interesting to notice is that the distillation mechanism goes together with the density-dependent behavior of the isovector variances described just above. As shown by Figs. 1 and 2, large density
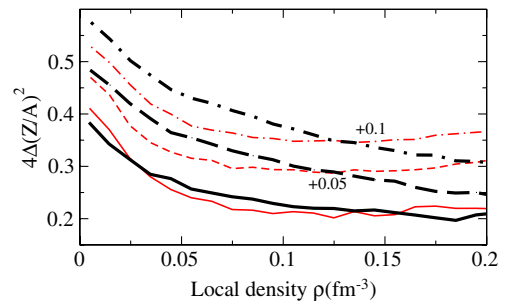

FIG. 2 (color online). The quantity $4\Delta(\overline{Z/A})^2$ (see text) is plotted as a function of the local density, for systems having initial density ρ_1 (full lines), ρ_2 (dashed lines), ρ_3 (dot-dashed lines). Curves are shifted for a better visibility. Black, asy-stiff EOS; gray (red), asy-soft EOS.

domains are associated with larger F_{eff}^{v} (i.e., smaller fluctuation width $\sigma_{\rho^{v}}/\rho$) and smaller asymmetry, whereas low-density regions are on average more asymmetric but also more fluctuating.

Let us move to study the probability $Y(Z, N)$ to find, inside a volume V, a given number of protons and neutrons, $Z = \rho_{n,V} V$ and $N = \rho_{p,V} V$. $\rho_{n,V}$ and $\rho_{p,V}$ denote neutron and proton densities averaged over V, whose sum yields the density ρ_V. Here we consider $V = (5.5 \text{ fm})^3$. The quantity $Y(Z, N)$ is proportional to the probability of getting, in the volume V, a specific variation of the isovector density ρ^v, with respect to the average $\bar{\rho}^v$: $P(\rho^v) \approx$ $\exp-(\rho^v - \bar{\rho}^v)^2/(2\sigma_{\rho^v})$. Using the identity $\rho^v/\rho_V = I = (N - Z)/A$ and considering the equilibrium amplitude of σ_{ρ^v} [see Eqs. (3) and (4)], one can write, for the yield ratio between systems (1) and (2),

$$\ln(Y_2/Y_1) \approx [(I - \bar{I}_1)^2 - (I - \bar{I}_2)^2] A F_{\mathrm{eff}}^v / T, \quad (5)$$

where F_{eff}^v and the average asymmetry $\bar{I}_i$ are functions of ρ_V (in our case $\bar{I}_1 = 0$). We notice that the ratio Y_2/Y_1 does not depend explicitly on the volume V. After some algebra, Eq. (5) can be rewritten as

$$\ln(Y_2/Y_1) \approx [(\bar{I}_1^2 - \bar{I}_2^2)(N + Z) - 2(\bar{I}_1 - \bar{I}_2)(N - Z)] F_{\mathrm{eff}}^v / T. \quad (6)$$

Expressing $\bar{I}_i$ in terms of the average proton or neutron fraction, we finally get $\ln(Y_2/Y_1) \approx \alpha N + \beta Z$, with

$$\begin{aligned} \alpha(\rho_V) &= 4\Delta(\overline{Z/A})^2 F_{\mathrm{eff}}^v / T, \\ \beta(\rho_V) &= 4\Delta(\overline{N/A})^2 F_{\mathrm{eff}}^v / T. \end{aligned} \quad (7)$$

Thus we recover the standard isoscaling relations [20], but with density-dependent coefficients $\alpha(\rho_V)$ and $\beta(\rho_V)$, linked to the effective symmetry free energy F_{eff}^v.

The behavior of the exponent α is illustrated in Fig. 3, where we plot the quantity $\ln(Y_2/Y_1)$ as a function of N, for the charges $Z = 1$–10. In spite of the implicit density dependence of the isoscaling parameters, we note that the slope α is the same for all charges. This result follows from the opposite trend, shown by Figs. 1 and 2, of the two quantities $\Delta(\overline{Z/A})^2$ and F_{eff}^v, so that the product remains almost constant (see the inset of Fig. 3). More precisely, the quantities $\Delta(\overline{Z/A})^2$ and $\Delta(\overline{N/A})^2$ go approximately as $\frac{\rho_0}{\rho} \frac{\partial C_{\mathrm{sym}}}{\partial \rho}|_{\rho = \rho_0}$ [31], counterbalancing the density dependence of F_{eff}^v. In the case of a linear behavior of F_{eff}^v, i.e., close to the conditions of our stiff case, the isoscaling parameters, Eq. (7), would be exactly constant. However, also in the soft case (not shown in the figure), the exponent α is roughly the same for all Z values (within 7%.) Within our framework, the nearly constant value of α (or β) inside the fragmenting system could be at the origin of the experimental observation of the same isoscaling parameter for the several products issued from nuclear reactions [21], which in principle may originate from different density
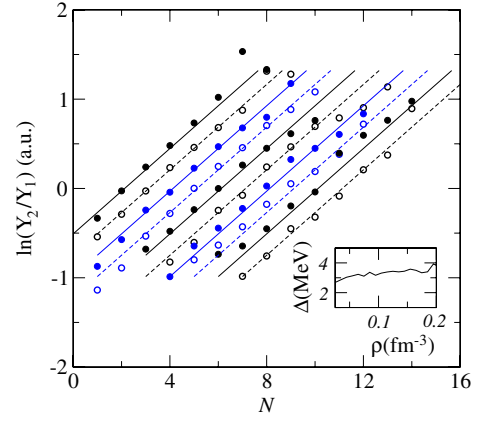

FIG. 3 (color online). The quantity $\ln(Y_2/Y_1)$ is plotted as a function of N, for the charges $Z = 1$–10, in the case of the systems with initial density ρ_1. The stiff parametrization is considered. Lines are to guide the eye. The inset shows the product $\Delta = 4\Delta(\overline{Z/A})^2 F_{\mathrm{eff}}^v$, as a function of the local density.

regions and/or have different average density. Then, knowing α (or β) and the average asymmetry of a considered reaction product, Eq. (7) gives the corresponding effective symmetry energy of the density region from which it emerges. In other words, this analysis allows one to probe the local symmetry energy of clusterized systems. It should be noted that this provides different information with respect to the extraction of the total symmetry energy associated with clusterized low-density matter [14,32].

To conclude, in this Letter we have undertaken a dynamical study of the disassembly of two-component unstable systems, focusing on the coupling between the development of isoscalar and isovector density fluctuations. For nuclear systems, we have shown that the amplitude of isovector fluctuations follows the evolution of the local density and approaches, within time scales compatible with nuclear reactions at Fermi energies, the corresponding local equilibrium value that is linked to the density-dependent symmetry free energy. Thus, fragment isospin fluctuations and isoscaling parameters are related to the symmetry energy at the fragment formation density. These results are relevant to experimental isoscaling analyses aiming at extracting information on the symmetry energy, a current topic of strong interest in nuclear physics and astrophysics [12,17,33–37]. Though secondary decay effects are expected to reduce the sensitivity of these observables to the specific shape of the symmetry energy [37], this analysis should still allow one to probe the range of values spanned within the low-density conditions reached in nuclear fragmentation reactions. Finally, it should be noted that our study is performed within the semiclassical approximation. It would be interesting to introduce quantum fluctuations and investigate their influence on the relation between isoscaling, isotopic distributions, and symmetry energy.

[1] Y. E. Kim and A. L. Zubarev, Phys. Rev. A **70**, 033612 (2004).

[2] M. Schmidt, R. Kusche, B. von Issendorff, and H. Haberland, Nature (London) **393**, 238 (1998); C. Hock, C. Bartels, S. Straßburg, M. Schmidt, H. Haberland, B. von Issendorff, and A. Aguado, Phys. Rev. Lett. **102**, 043401 (2009).

[3] L. G. Moretto, J. B. Elliott, L. Phair, and P. T. Lake, J. Phys. G **38**, 113101 (2011).

[4] A. Smerzi, A. Trombettoni, P. Kevrekidis, and A. Bishop, Phys. Rev. Lett. **89**, 170402 (2002).

[5] N. Chamel and S. Goriely, Phys. Rev. C **82**, 045804 (2010).

[6] F. Matera, Phys. Rev. A **68**, 043624 (2003).

[7] H. Muller and B. D. Serot, Phys. Rev. C **52**, 2072 (1995).

[8] G. Bertsch and P. J. Siemens, Phys. Lett. **126B**, 9 (1983).

[9] D. R. Bowman, G. F. Peaslee, R. T. DeSouza et al., Phys. Rev. Lett. **67**, 1527 (1991).

[10] B. Borderie and M. F. Rivet, Prog. Part. Nucl. Phys. **61**, 551 (2008), and references therein.

[11] Ph. Chomaz, M. Colonna, and J. Randrup, Phys. Rep. **389**, 263 (2004).

[12] M. B. Tsang et al., Prog. Part. Nucl. Phys. **66**, 400 (2011).

[13] D. V. Shetty, S. J. Yennello, and G. A. Souliotis, Phys. Rev. C **76**, 024606 (2007).

[14] G. Lehaut, F. Gulminelli, and O. Lopez, Phys. Rev. Lett. **102**, 142503 (2009).

[15] E. Galichet, M. Colonna, B. Borderie, and M. Rivet, Phys. Rev. C **79**, 064615 (2009).

[16] F. Amorini et al., Phys. Rev. Lett. **102**, 112701 (2009).

[17] J. M. Lattimer and M. Prakash, Phys. Rep. **442**, 109 (2007); A. W. Steiner, J. M. Lattimer, and E. F. Brown, Astrophys. J. **722**, 33 (2010).

[18] C. Ducoin, J. Margueron, C. Providência, and I. Vidaña, Phys. Rev. C **83**, 045810 (2011).

[19] A. Carbone, G. Colò, A. Bracco, L.-G. Cao, P. F. Bortignon, F. Camera, and O. Wieland, Phys. Rev. C **81**, 041301 (2010).

[20] A. S. Botvina, O. V. Lozhkin, and W. Trautmann, Phys. Rev. C **65**, 044610 (2002).

[21] M. B. Tsang, W. A. Friedman, C. K. Gelbke, W. G. Lynch, G. Verde, and H. S. Xu, Phys. Rev. Lett. **86**, 5023 (2001).

[22] A. Le Fevre et al., Phys. Rev. Lett. **94**, 162701 (2005).

[23] S. Ayik and C. Gregoire, Phys. Lett. B **212**, 269 (1988); Nucl. Phys. **A513**, 187 (1990).

[24] J. Rizzo, Ph. Chomaz, and M. Colonna, Nucl. Phys. **A806**, 40 (2008), and references therein.

[25] M. Colonna, M. Di Toro, A. Guarnera, S. Maccarone, M. Zielinska-Pfabé, and H. H. Wolter, Nucl. Phys. **A642**, 449 (1998).

[26] C. J. Pethick and D. G. Ravenhall, Ann. Phys. (N.Y.) **183**, 131 (1988).

[27] L. D. Landau and E. M. Lifshitz, *Statistical Physics, Part 1* (Butterworth-Heinemann, Oxford, 1980), 3rd ed., Vol. 5.

[28] V. Baran, M. Colonna, M. Di Toro, V. Greco, M. Zielinska-Pfabé, and H. H. Wolter, Nucl. Phys. **A703**, 603 (2002).

[29] V. Baran, M. Colonna, V. Greco, and M. Di Toro, Phys. Rep. **410**, 335 (2005).

[30] M. Colonna, M. Di Toro, and A. Guarnera, Nucl. Phys. **A589**, 160 (1995).

[31] M. Colonna and F. Matera, Phys. Rev. C **77**, 064606 (2008).

[32] S. Typel, G. Röpke, T. Klähn, D. Blaschke, and H. H. Wolter, Phys. Rev. C **81**, 015803 (2010).

[33] Ad. R. Raduta and F. Gulminelli, Phys. Rev. C **75**, 024605 (2007).

[34] S. R. Souza and M. B. Tsang, Phys. Rev. C **85**, 024603 (2012).

[35] C. A. Dorso, P. A. Gimenez Molinelli, and J. A. Lopez, J. Phys. G **38**, 115101 (2011).

[36] P. Marini et al., Phys. Rev. C **85**, 034617 (2012).

[37] A. Ono, P. Danielewicz, W. A. Friedman, W. G. Lynch, and M. B. Tsang, Phys. Rev. C **70**, 041604 (2004).